AlGaSb/GaSb-based Metal-Semiconductor-Metal and *p-i-n* Photodetectors

Y. Wang, K. Longenbach, M. C. Teich, and W. I. Wang
Department of Electrical Engineering
Columbia University, New York, NY 10027

S. Tiwari, and M. C. Hargis
IBM Thomas J. Watson Research Center, Yorktown Heights, NY 10598

GaSb-based metal-semiconductor-metal (MSM) and *p-i-n* photodetectors grown by molecular beam epitaxy have been demonstrated for the first time. These novel devices can offer higher bandwidths and lower excess noise because of the superior hole transport properties of GaSb and the enhanced hole ionization rate of AlGaSb alloys. MSM photodetectors employing GaSb active region and AlGaSb barrier-enhancing abrupt region are grown on InP substrates, while p-i-n photodiodes are grown on GaSb substrates. These MSM detectors exhibit photoresponse in the range of 0.2-0.65 A/W and a 3 dB bandwidth exceeding 1 GHz at 300 K and 10 GHz at 77 K. The dark currents of ~ 10^{-6} A at 300 K and ~ 10^{-10} A at 77 K are measured for 25 x 25 devices. The p-i-n photodiodes have breakdown voltages as high as 20 V. The leakage currents of these devices are 60 μA at half the breakdown voltage and 10 μA after nitrogen plasma passivation for 40 x 40 devices. To the best of our knowledge, these are the best results obtained from the structures grown by MBE.

0-8194-0841-7/92/$4.00

$Ga_{0.47}In_{0.53}As$ has been the III-V semiconductor most widely investigated for 1.3 μm and 1.5 μm MSM photodetectors because of the relative ease with which they can be monolithicly integrated with GaInAs/InP based high speed LSIs [1, 2]. However, these devices exhibit large bandwidths only when they are biased at large voltages. These large bias voltages are necessary to enhance the hole velocity as well as hole emission across the metal-semiconductor barrier region. Optimum performance of these devices requires the compromise of a lower barrier height which increases the dark current, in order to achieve smaller hole pile-up together with efficient hole collection. Thus, hole transport and storage are very important factors in the optimum operation of MSM photodetectors. Recently considerable attention has been paid to the GaSb/AlSb material system as an alternative to the InGaAs/InP system for use as 1.3 μm and 1.5 μm photodetectors [3,4], because of the superior hole transport properties of GaSb. Up to now, no research has been done on the use of GaSb for MSM photodetectors. Unlike that at InGaAs surface, the Fermi level at GaSb surface pins closer to the valence band, which may lead to higher dark current. However, the dark current can be significantly reduced by the use of the barrier-enhancing $Al_{1-x}Ga_xSb/GaSb$ heterostructure, while retaining the lower effective hole mass of the GaSb-based alloy system. The use of this structure results in improved hole collection and higher hole velocity. Since this material system is lattice matched to InAs, it offers the possibility of integration with InAs n-channel as well as complementary FETs [5, 6]. Furthermore, the enhanced hole ionization rate in AlGaSb alloys with small Al fraction, which is a result of the direct match between its bandgap and the spacing of the spin orbital split-off band, enables the GaSb/AlGaSb avalanche photodiodes (APDs) to have lower excess noise than the widely used InGaAs/InP APDs.

The MSM structure reported here consists of a semi-insulating InP substrate, a 1.5 μm GaSb active layer, a 500 Å $Al_{0.5}Ga_{0.5}Sb$ barrier layer, and finally a 50 Å GaSb thin cap layer. All of these layers were doped with PbTe to achieve lightly n-type material. Interdigitated-finger structures with finger lengths and finger spacings from 1 to 4 μm and finger widths

varying from 25 to 90 μm were fabricated using silicon nitride as a dielectric layer, aluminum as a metal barrier, and titanium-platinum-gold as the interconnect metal. Fig. 1 shows the modulation response at room temperature for a large area detector at a wavelength of 1.3 μm. The 3 dB response bandwidths of the device exceed 1.0 GHz at a bias voltage of 2.5 V. The devices exhibit dark currents of ~ 1 μA at the same bias voltage. The bandwidths are similar to those observed in similarly structured $Ga_{0.47}In_{0.53}As$ MSM detectors at similar bias voltages.

However, a significant improvement in response does occur near 77 K as shown in Fig. 2. The laser has a full-width-half-maximum (FWHM) of ~ 23 ps and the photodetector has a FWHM of ~ 27 ps. This indicates an increase in hole mobility which leads to an improvement in the detector response in the initial part of the carrier collection process. The tail of this response corresponds to a velocity of ~ 3×10^6 cm s^{-1} at an electric field of 2.5×10^3 Vcm^{-1}. The bandwidth of the detector, based on these measurement, exceeds 10 GHz at the bias voltage of 5 V. This is a substantial improvement over $Ga_{0.47}In_{0.53}As$ MSM detectors which typically have bandwidths of about 3-4 GHz under the same bias conditions. This low temperature response suggests an improvement in the characteristics of the detectors and can be attributed to the improvements in transport and storage of holes in these structures. The decrease in FWHM, largely associated with the peak response region and hence with high carrier densities in the detector, suggests both an improvement in the low-field velocity of carriers which occurs due to improvements in mobility, and the insignificant effect of collection inefficiencies at these large hole carrier densities. At 300 K, the mobilities in these structures are still low, similar to those of other III-V semiconductors, which is perhaps due to the effects of residual defects arising from the lattice-mismatched growth and residual impurities.

The highly efficient collection of holes in this device suggests that the effective barrier height of these structures is probably small. Fig. 3 shows the activation energy plots of the conductance at zero bias for three different area devices. The activation energies of these structures are in the range of 0.27-0.30 eV. Since these are n-type structures, the activation energies

should correspond to electron transport. The bandgap of $Ga_{0.5}Al_{0.5}Sb$ material is about 1.3 eV with the X-minimum as the lowest valley. The conduction band and valence band offset in the $GaSb/Ga_{0.5}Al_{0.5}Sb$ system are quite symmetric, approximately 0.20-0.25 eV for both barriers. The barrier height of the metal-$Ga_{0.5}Al_{0.5}Sb$ system is expected to be ~ 0.7 eV. The discrepancy of the predicted with the measured effective barrier height may come from a low-activation conduction process, such as from defects due to the lattice-mismatched growth on InP substrates.

In Fig. 4 the responsivity of the detectors, at 300 K is presented as a function of optical intensity for various bias voltages. At low bias voltages, the responsivity is about 0.2 A/W; at high bias voltages, it can exceed 0.6 A/W which is close to the theoretical maximum. The intensity dependence of the responsivity is large at high bias voltages and is attributed to both the low frequency gain and the limitations on transport placed by an abrupt barrier. The use of graded junctions should decrease the latter effect.

$Al_{0.06}Ga_{0.94}Sb/GaSb$ *p-i-n* diode structures have also been grown under the same conditions as were the above MSM detectors. These p-i-n diode structures were grown on n^+ GaSb substrates and consist of a 2 μm unintentionally doped $Al_{0.06}Ga_{0.94}Sb$ layer followed by a 1μm Be doped p^+ GaSb layer. Standard wet etching techniques were used to form the diode mesas. Ni and Au were evaporated to make front contacts on the p^+ GaSb epilayer. These diodes exhibit breakdown voltages as high as 20 V and leakage currents of 60 μA at one half the breakdown voltage for 40 x 40 μm^2 devices. As far as we know, these are the best results achieved by GaSb based diodes grown by MBE. In order to suppress the leakage current, we have studied the effect of surface cleaning and passivation by hydrogen and nitrogen plasmas produced by an electron cyclotron resonance (ECR) plasma source. Immediately after hydrogen plasma cleaning, the leakage current was measured at 10 μA. However, after several days exposure to air the leakage current increased. In order to maintain a low leakage current, we experimented with nitrogen plasma passivation. We found that after this procedure the leakage current of a p-i-n diode remained at virtually the same low value after several days exposure to the air. Fig. 5

shows the I-V curves of the diode before the plasma treatment and after hydrogen plasma cleaning and nitrogen plasma passivation.

In conclusion, we have reported an initial demonstration of GaSb MSM photodetectors and GaSb/$Al_{0.06}Ga_{0.94}Sb$ p-i-n diodes with high breakdown voltages. We have also demonstrated substantial improvements in suppressing leakage currents through the use of plasma treatments. These devices may be suitable for long wavelength detection applications. We have also presented evidence, based on low temperature measurements, that the MSM detectors exhibit the properties expected to arise from improvement in hole transport.

We would like to thank Z.Lu and R. Osgood for help with the ECR plasma treatments. This work is supported by the National Science Foundation and NCIPT/DARPA.

References

[1] J. B.Soole, H. Schumacher, H. P. Leblanc, R. Bhat, and M. A. Koza, IEEE Photon. Technol. Lett., **1**, 250, 1989.

[2] J. B. Burroughes and M. Hargis, IEEE photon. Technol. Lett., **3**, 532, 1991.

[3] O. Hildebrand, W. Kuebart, K. Benz, and M. Pilkuhn, IEEE J. Quantum Electron., **QE-17**, 284, 1981.

[4] M. Ichimura, K. Higuchi, Y, Hattori, and T. Wada, J. Appl. Phys. **68**, 6135, 1990.

[5] L. F. Luo, R. Bereford, W. I. Wang, and H. Munekata, Appl. Phys. Lett., **55**, 789, 1989.

[6] L. F. Luo, K. F. Longenbach, and W. I. Wang, IEEE Electron Device Lett. **EDL-11**, 567, 1990.

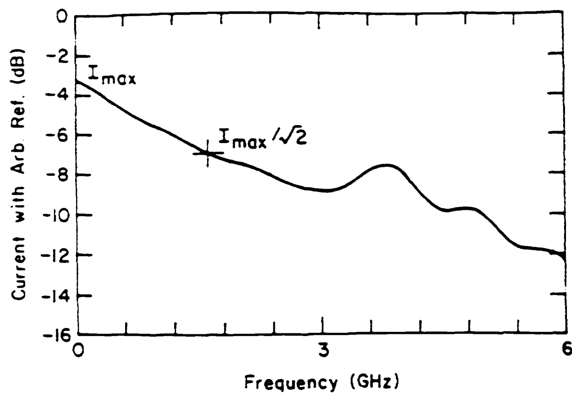

Fig . 1 The modulation response at 1.3 µm wavelengthand 2.5 V bias voltage for a 90x90 μm^2 MSM diode employing 2 µm finger length and spacing.

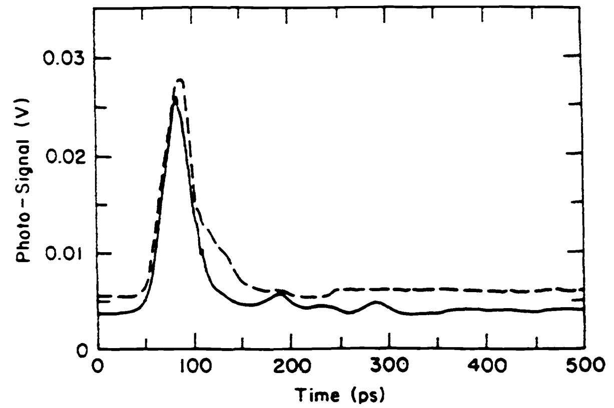

Fig. 2 The temporal response at 77 K to a laser pulse with FWHM of 23 ps. the solid line shows the detected laser signal and the dashed line shows the detector signal.

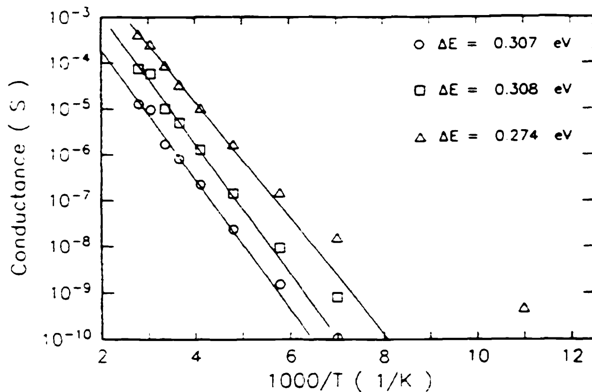

Fig. 3 Activation energy plots of zero-bias conductance for a 25x25 μm^2 area detector (circles), a 55x55 μm^2 area detector (sqares), and 90x90 μm^2 area detector (triangle) with equal finger lengths and spacings.

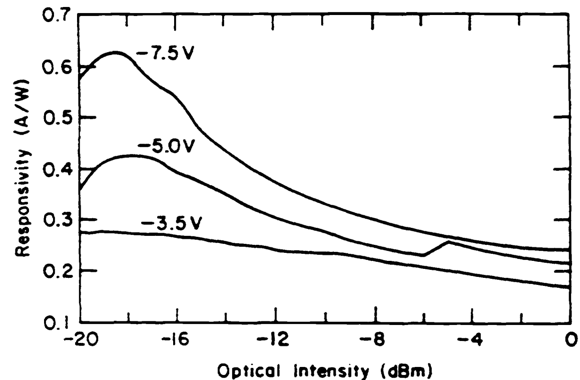

Fig. 4 Responsivity at 300 K as a function of optical intensity of 1.3 µm wavelength for various bias voltages.

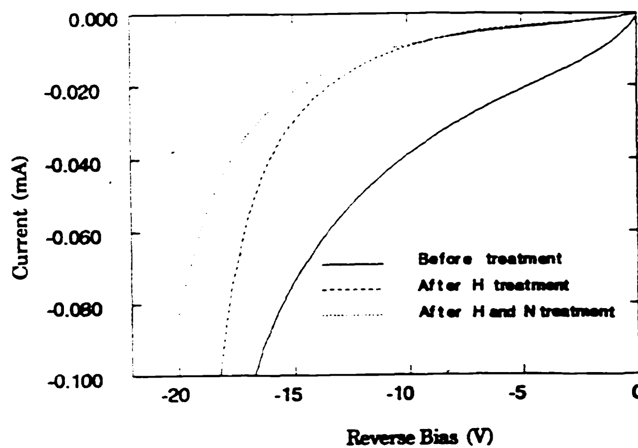

Fig. 5 Reverse I-V Measurement of a p-i-n diode.